Growth of nanostructured molybdenum disulfide (MoS₂) thin films on a nanohole-patterned substrate using plasma-enhanced atomic layer deposition (ALD)

Zhigang Xiao^{1*}, Gregory Doerk², Kim Kisslinger², Abram Jones¹, and Rebhadevi Monikandan³

¹Department of Electrical Engineering, Alabama A&M University, Normal, AL 35762, USA

²Center for Functional Nanomaterials, Brookhaven National Laboratory, Upton, NY 11973, USA

³Materials Characterization Facility, Georgia Institute of Technology, Atlanta, Georgia 30332, USA

*Corresponding Author: Zhigang Xiao; Email: zhigang.xiao@aamu.edu.

Abstract

Nanostructured molybdenum disulfide (MoS₂) thin films were grown on a nanohole-patterned silicon substrate using plasma-enhanced atomic layer deposition (ALD). A nanoscale hole-patterned silicon substrate was fabricated for the growth of MoS₂ film using the self-assembly-based nanofabrication method. The nanoscale holes can significantly increase the surface area of substrate while the formation and growth of nanostructures normally start at the surface of substrate. Hydrogen sulfide (H₂S) gas was used as the S source in the growth of molybdenum disulfide (MoS₂) while molybdenum (V) chloride (MoCl₅) powder was used as the Mo source. The MoS₂ film had the stoichiometric ratio of 1 (Mo) to 2 (S), and had the peaks of E^{1}_{2g} and A_{1g} which represent the in-plane and out-plane vibration modes of Mo-S bond, respectively. It was found that the MoS₂ film grown in the nanoscale hole, especially at the wall of hole has more hexagonal-like structures due to the effects of the nanoscale space confinement and nanoscale interface although the film shows an amorphous structure. A post-growth high-temperature annealing ranging from 800 °C to 900 °C produced local crystalline structures in the film, which are compatible with those reported by other researchers.

Key words: molybdenum disulfide (MoS₂), plasma-enhanced atomic layer deposition, self-assembly, nanofabrication.

1. Introduction

Transition metal dichalcogenides (TMD) nanomaterials such as 2D molybdenum disulfide (MoS₂) has attracted a lot of research interest in the past ten years due to their potential for the application of future nanoelectronic materials. 2D transition metal dichalcogenides (TMD) nanomaterials such as 2D molybdenum disulfide (MoS₂) are semiconductors with large bandgaps (\sim 1–2 eV) as well as moderate carrier mobilities (a few to hundreds of cm² V⁻¹ s⁻¹) [1, 2] and are ideal channel materials for the fabrication of high-performance field-effect transistors with high current on/off ratios [3]. Nanoelectronic devices built on 2D materials could revolutionize the future semiconductor technology [4-6]. However, the preparation of ultrathin 2D TMD nanomaterials is changeling. The chemical vapor deposition (CVD) could grow the 2D transition metal dichalcogenides (TMD) nanomaterials with desired compositions and enhanced electrical properties [7-9].

In this paper, the first research objective was to explore the growth of molybdenum disulfide (MoS_2) thin films using plasma-enhanced atomic layer deposition (PE-ALD) [10, 11]. It is important to find suitable precursors for the PE-ALD of MoS₂. Molybdenum (V) chloride $(MoCl_5)$ and molybdenum hexacarbonyl $(Mo(CO)_6)$) precursors were used by researchers as the Mo source in the growth of monolayer MoS_2 , while hydrogen disulphide (H_2S) and dimethyldisulfide $(C_2H_6S_2)$ precursors were used as the S source [12, 13]. Hydrogen sulfide (H_2S) was used as the S source in the growth of molybdenum disulfide (MoS_2) thin films while molybdenum(V) chloride $(MoCl_5)$ powder was used as the Mo source. Hydrogen sulfide (H_2S) has advantage over any other

available S-containing precursors as the S source for the growth of MoS₂, first, it is gas and can be easily introduced into the deposition chamber; second, it has only two elements (S and H) and can not introduce any additional elements into the MoS₂ film during the deposition. However, H₂S is toxic and also reactive to many materials including metals such as copper. In order to use the H₂S gas for the research, the ALD system was updated significantly and many parts of the system such as the valves and sealing O-rings were replaced with the H₂S-compatible parts. Molybdenum (V) chloride (MoCl₅) also has advantage over any other available Mo-containing precursors as the Mo source for the growth of MoS₂, it has only two elements (Mo and Cl) and can not introduce any additional elements into the MoS₂ film during the deposition. In addition, although molybdenum (V) chloride (MoCl₅) is a powder, it only needs to be heated to about 70 °C to obtain enough vapor pressure for being introduced into the deposition chamber [12].

The second research objective was to investigate the effect of nanoscale interface on the growth of molybdenum disulfide (MoS₂) thin films using the nanoscale hole-patterned silicon substrate. A silicon substrate was fabricated and patterned with uniform nanoscale holes using the self-assembly-based nanofabrication method for the growth of MoS₂ film [14-17]. It was expected that the nanoscale hole could enhance the formation of MoS₂ hexagonal-like structures in the hole, because the nanoscale holes can significantly increase the interfacial area of film with the substrate due to the large wall surface of holes compared to their volume, the formation and growth of nanostructures and crystal structures normally start at the interface of film with the substrate, more interface produce more nanostructures. It was found that the film grown in the nanoscale hole demonstrated more hexagonal-like structures, especially more hexagonal-like

structures appeared near the wall of holes. A post-growth high-temperature annealing at 800 °C or 900 °C in the environment of argon (Ar) for 8 min produced local crystalline structures in the film randomly, which are compatible with the results reported by other researchers [13, 18, 19].

2. Experimental Details

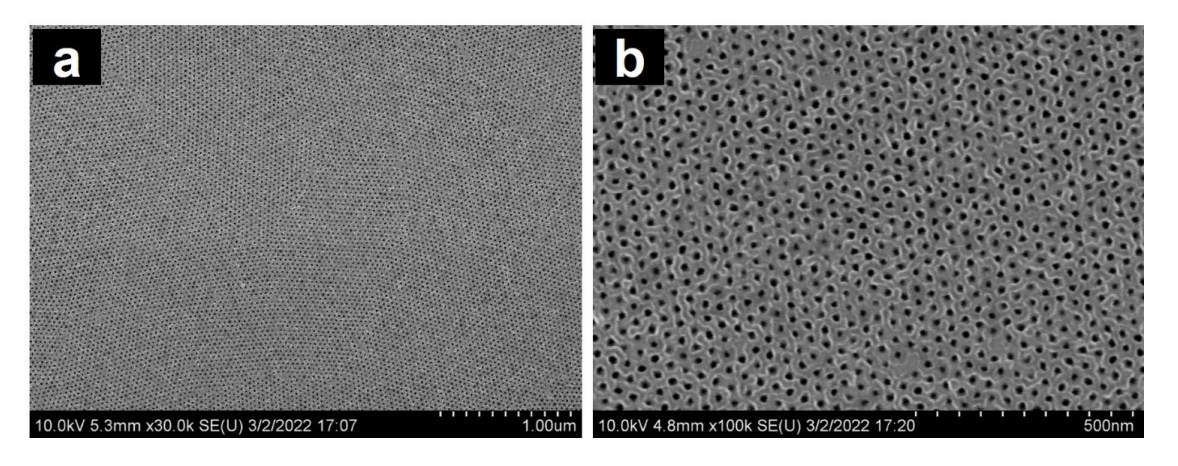


Figure 1. (a) SEM image of a fabricated nanoscale-hole silicon substrate; (b) Enlarged view of the fabricated nanoscale-hole substrate, the diameter of the nanoscale holes is about 20 nm – 30nm and the depth of the nanoscale holes is about 120 nm – 160 nm.

Figures 1(a) and (b) show the SEM image of the fabricated nanoscale-hole silicon substrate. The diameter of the nanoscale holes is about 20 nm – 30nm and the depth of the nanoscale holes is about 120 nm – 160 nm. Hexagonal nanopatterns used for hole fabrication were formed through self-assembly of a thin film of polystyrene-block-poly(methyl methacrylate) (PS-b-PMMA) diblock copolymer blended with PS and PMMA homopolymers. Cylinder-forming asymmetric PS-b-PMMA ($M_n = 46.1$ -b-21 kg/mol, $M_w/M_n = 1.09$), homopolymer PS ($M_n = 3.5$ kg/mol, $M_w/M_n = 1.05$) and homopolymer PMMA ($M_n = 3$ kg/mol, $M_w/M_n = 1.14$) were purchased from Polymer Source Inc. A hydroxyl-terminated random copolymer "neutral" brush of PS and PMMA provided by the Dow Chemical Company (P(S-r-PMMA)-OH; 69% styrene, determined by 13 C NMR 21 dissolved in

U

propylene glycol monomethyl ether acetate (PGMEA) and was diluted to a concentration of 1% (w/w). All other polymers were dissolved in toluene at 2% (w/w). A blend solution was prepared by mixing the PS-*b*-PMMA, PS, and PMMA solutions in a 60:28:12 weight ratio. This blend was used due to the enhanced self-assembly kinetics afforded by the added homopolymer [14, 15].

A silicon wafer was first cleaned by exposure to oxygen plasma for 60s at 100 mTorr and 20 W (March Plasma CS1701F). The random copolymer brush was then grafted to the oxidized silicon surface to form a neutral underlayer as described previously [16]. Briefly, a random copolymer film is spin coated onto the clean silicon wafer at 1500 rpm to obtain a film 20-30 nm thick. The wafer is then thermally annealed at 250 °C for 5 min under continuous nitrogen purging to ensure the chemical grafting of the material. Excess ungrafted polymer is removed by spin-rinsing in PGMEA at 3000 rpm. The block copolymer/homopolymer blend was then spun onto the wafer at 3000 rpm, yielding a ~70 nm thick film, which was then thermally annealed at 250 °C for 5 min under continuous nitrogen purging to promote self-assembly. PMMA degradation was accomplished by UV irradiation for 10 minutes from a low pressure mercury arc lamp (G10T5 1/2VH, Atlantic Ultraviolet Corporation) in a closed chamber purged by continuously flowing nitrogen. The incident power was ~8 mW/cm² at the sample position at a wavelength of 254 nm. Degraded PMMA was then selectively removed by immersing the sample in acetic acid for 5 min and subsequently in deionized water for 3 minutes, yielding a PS film with ordered arrays of vertically oriented nanopores. Oxygen plasma etching for 10 s at 20W was performed to remove remaining random copolymer at the substrate surface inside the pores.

Holes in silicon were then fabricated through reactive ion etching in an Oxford PlasmaLab 100 using the porous PS film as a mask. As described previously [17], this pattern transfer by reactive ion etching employed a 44:11 combination of chlorine and oxygen gas for 80 s at 9 mTorr, with 40 W from a radio frequency (RF) electrode power source, and 250 W power from an inductively coupled plasma (ICP) RF power source. An initial 8 s high power etch step (10 mTorr, 100 W RF power and 800 W ICP power) using a 20:5 combination of boron trichloride and chlorine gas was included to break through the native silicon oxide at the substate surface. Remaining PS from the mask film was removed using oxygen plasma (for 120 s at 20 W, 100 mTorr; March Plasma CS1701F).

A plasma enhanced atomic layer deposition system was used to grow the molybdenum disulfide (MoS₂) film in this research [10, 11]. Hydrogen sulfide (H₂S) was used as the S source in the growth of molybdenum disulfide (MoS₂) while molybdenum (V) chloride (MoCl₅) powder was used as the Mo source. In order that the H₂S gas can be used with the ALD system for the research, the system was updated significantly by the ALD Group of Kurt J. Lesker Company with the H₂S gas-compatible parts including the valves and sealing O-rings. The molybdenum(V) chloride (MoCl₅) powder was loaded in a stainless-steel bubbler which was designed with the flowing of carrier gas through it. The bubbler was heated at the temperature of 90 °C and was introduced into the process chamber with the carrier gas of argon (Ar). The sample was heated at 400 °C during the growth of MoS₂ thin film. The nanoscale hole-patterned silicon substrate was cleaned by the Ar plasma gas at 400 W for 20 cycles before the growth of the MoS₂ film. The deposition pressure was maintained at 1 Torr during the deposition. The cycle time was set as: 100 ms for

MoCl₅, 1000 ms for Ar purge, 1000 ms for Ar plasma, and 50 ms for H₂S. The MoS₂ film was grown for 200 cycles. The MoS₂ film was finally annealed at 800 °C or 900 °C for 8 min in a furnace with the flowing of argon (Ar) gas. The scanning electron microscope (SEM) was used to analyze the surface of the substrate and film while the high-resolution tunnel electron microscope (HRTEM) was used to analyze the cross-sectional structure of the MoS₂ film. The X-ray photoelectron spectroscopy (XPS) was used to analyze the compositions of the film and the Raman spectroscopy was used to analyze the Mo-S bond in the MoS₂ film [10].

3. Results and Discussion

Figure 2(a) shows the MoS_2 film grown on the nanoscale-hole silicon substrate. Figure 2(b) is an enlarged view of the surface of the substrate with MoS_2 on it. The MoS_2 film on the surface of substrate is about 20 nm think. Figure 2(a) and (b) present a relatively rough surface of substrate after the growth of MoS_2 compared to the surface of substrate before the growth of MoS_2 in Figure 1(a) and (b).

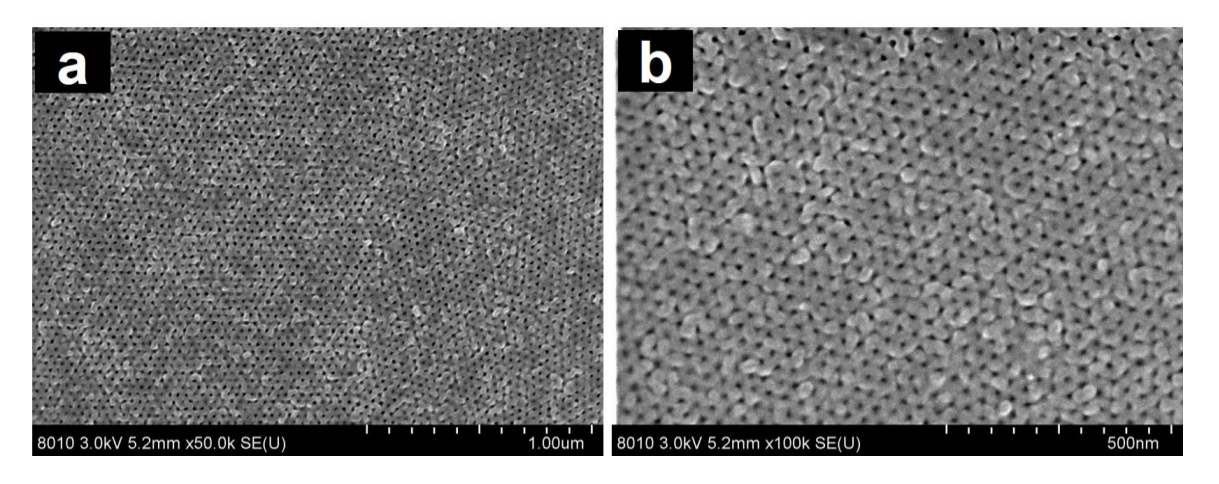


Figure 2. (a) SEM image of the nanoscale-hole silicon substrate after the growth of MoS_2 film on it; (b) Enlarged view of the nanoscale-hole substrate with MoS_2 film on it.

Figure 3 shows the cross-sectional TEM micrograph of the nanoscale-hole sample with MoS_2 film on it. The nanoscale hole fabricated with the self-assembly-based nanofabrication method has a diameter of about 20 nm – 30nm on the top with an inverted pyramid-like bottom and the depth of the nanoscale holes is about 120 nm – 160 nm. The holes were uniformly filled with the MoS_2 film and show a clear interface between the silicon substrate and MoS_2 film. The nanoscale hole has a large interfacial area of film with the substrate due to the large wall surface of hole compared to its volume.

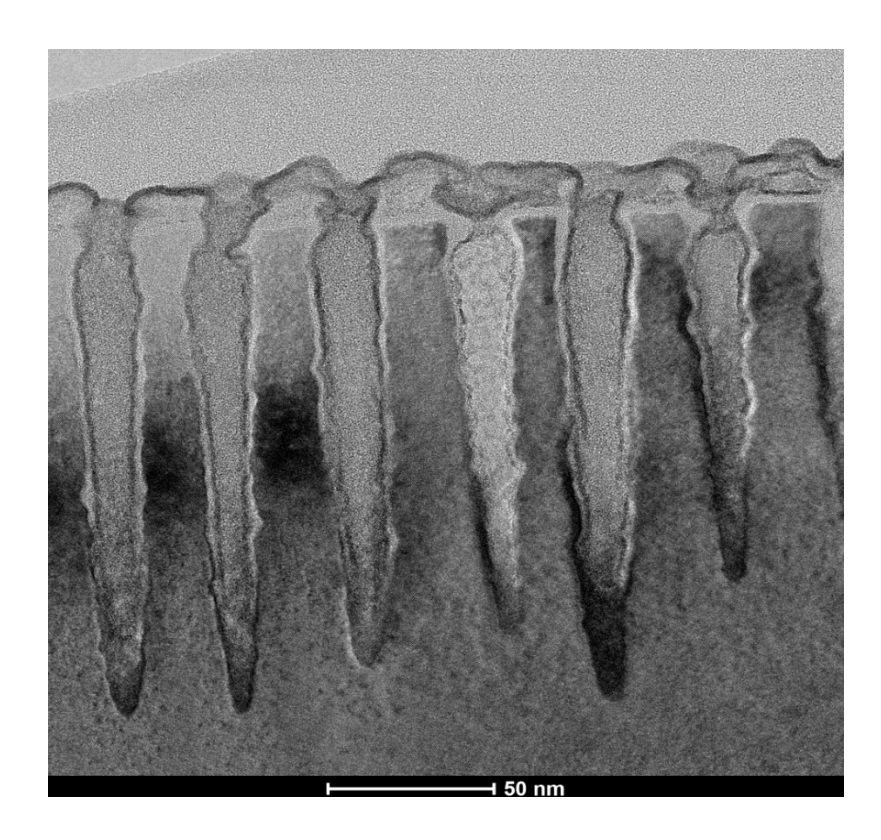


Figure 3. Cross-sectional TEM micrograph of the nanoscale hole-patterned silicon substrate with MoS_2 grown on it, showing that the nanoscale holes have a diameter of about 20 nm – 30nm on the top with an inverted pyramid-like bottom and the depth of the nanoscale holes is about 120 nm – 160 nm.

Figure 4(a) shows the cross-sectional HRTEM micrograph of the MoS_2 film in a nanoscale silicon hole without being annealed; Figure 4(b) is an enlarged view of the MoS_2 film grown on the outside surface of substrate, showing a pure amorphous structure; Figure 4(c) is an enlarged view of the MoS_2 film grown in the nanoscale hole, showing an amorphous structure with some hexagonal-like structures; Figures 4(d) and (e) are enlarged views of the MoS_2 film grown at the wall interface of the nanoscale hole, showing an amorphous structure, but with some clear hexagonal-like structures, which indicates that the nanoscale hole could enhance the formation of hexagonal-like structures, especially at the wall surface of hole, due to the nanoscale space confinement.

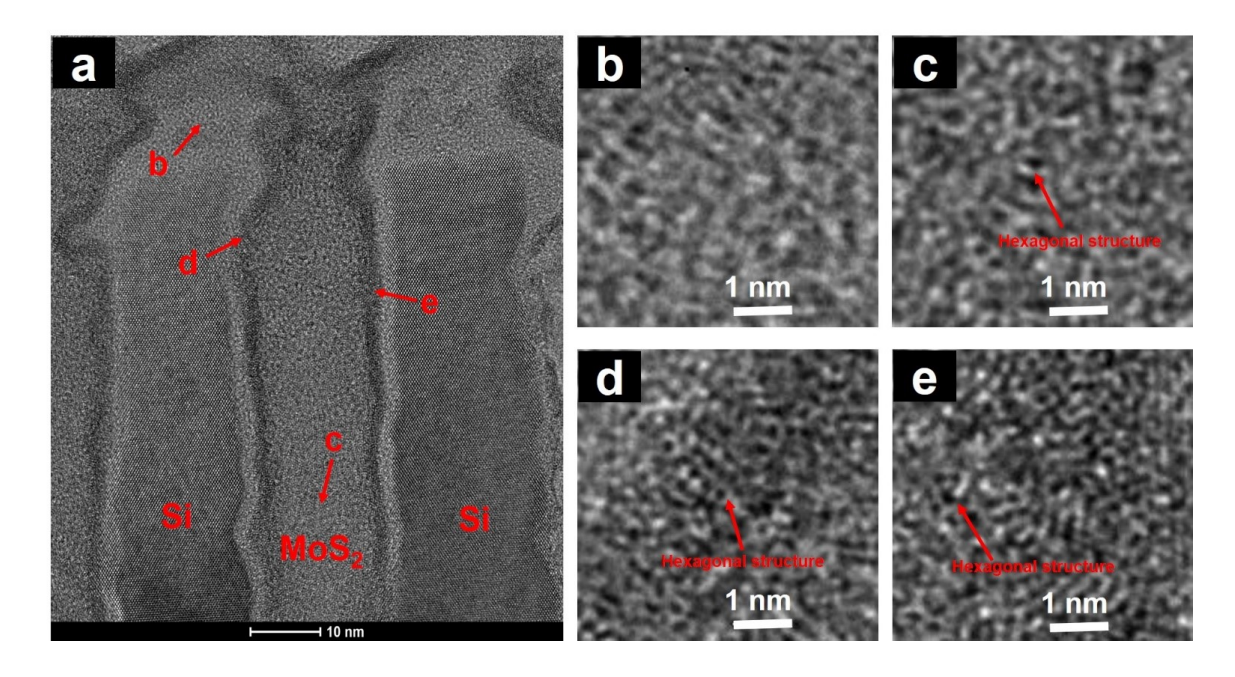


Figure 4. (a) HRTEM micrograph of the MoS_2 film grown in a nanoscale silicon hole; (b) the enlarged view of the MoS_2 film on the surface of substrate outside the hole marked by "b" in Figure 4 (a); (c) the enlarged view of the MoS_2 film in the nanoscale silicon hole marked by "c"; (d) the enlarged view of the MoS_2 film at the wall interface of hole marked by "d"; (e) the enlarged view of the MoS_2 film at the wall interface of hole marked by "e".

_

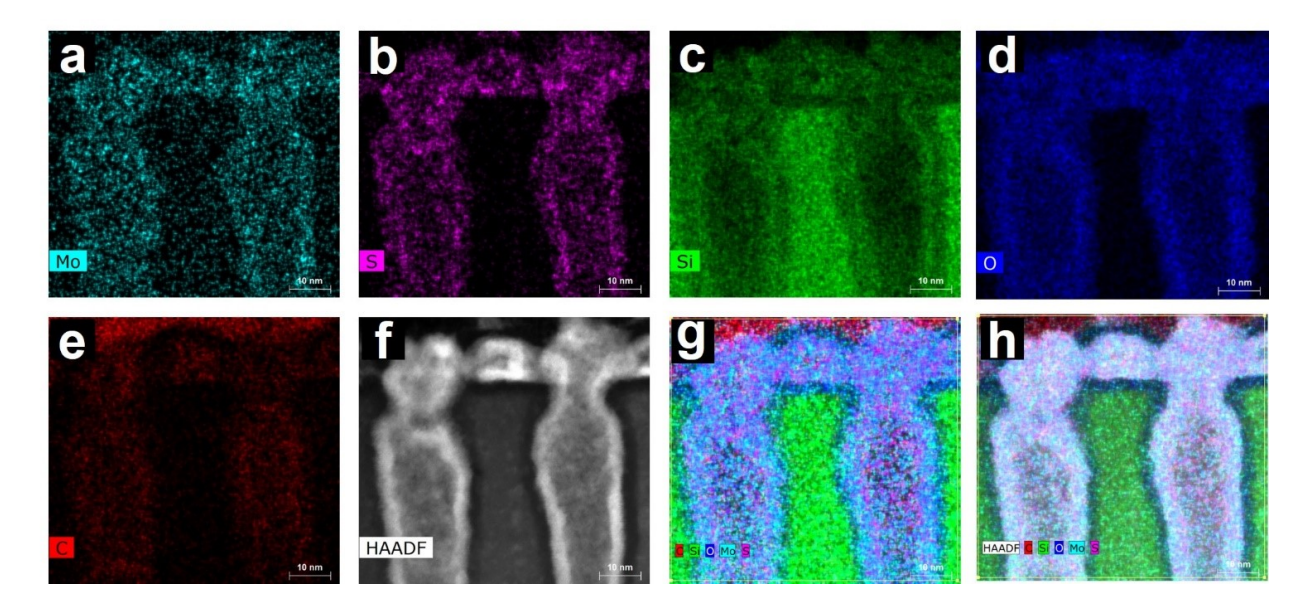


Figure 5. Color-coded EDS elemental maps of the nanoscale hole-patterned silicon substrate with the MoS2 film grown on the surface and inside the holes, where the color represents the corresponding element's K-alpha x-ray signal: (a) Molybdenum (Mo); (b) Sulfide (S); (c) Silicon (Si); (d) Oxygen (O); (e) Carbon (C); (f) HAADF STEM micrograph of the sample; (g) Combined color map with all the elements; (h) Combined color map with all the elements and the HAADF.

Figures 5(a)-(h) show the energy dispersive spectroscopy (EDS) elemental map analysis of the nanoscale hole-patterned silicon sample with the MoS₂ film inside the nanoscale holes, where the color represents the corresponding element's K-alpha x-ray signal: (a) Molybdenum (Mo); (b) Sulfide (S); (c) Silicon (Si); (d) Oxygen (0); (e) Carbon (C); (f) High-angle annular dark field (HAADF) STEM imaging of the sample; (g) Combined color map with all the elements; (h) Combined color map with all the elements and the HAADF. Figures 5(a) and (b) indicate that the film in the nanohole was MoS₂ and the hole was filled by the MoS₂ film uniformly. The high-angle annular dark-field (HAADF) STEM micrograph shows the image of the element with a high atomic number (Z) such as metal, therefore, Figure 5(f) further present the image of Mo distribution in the hole. The oxygen (O) in Figure 5(d) was from the surface silicon dioxide while the silicon (Si)

in Figure 5(c) was from the silicon substrate. The carbon (C) in Figure 5(e) was from the substrate and film surface.

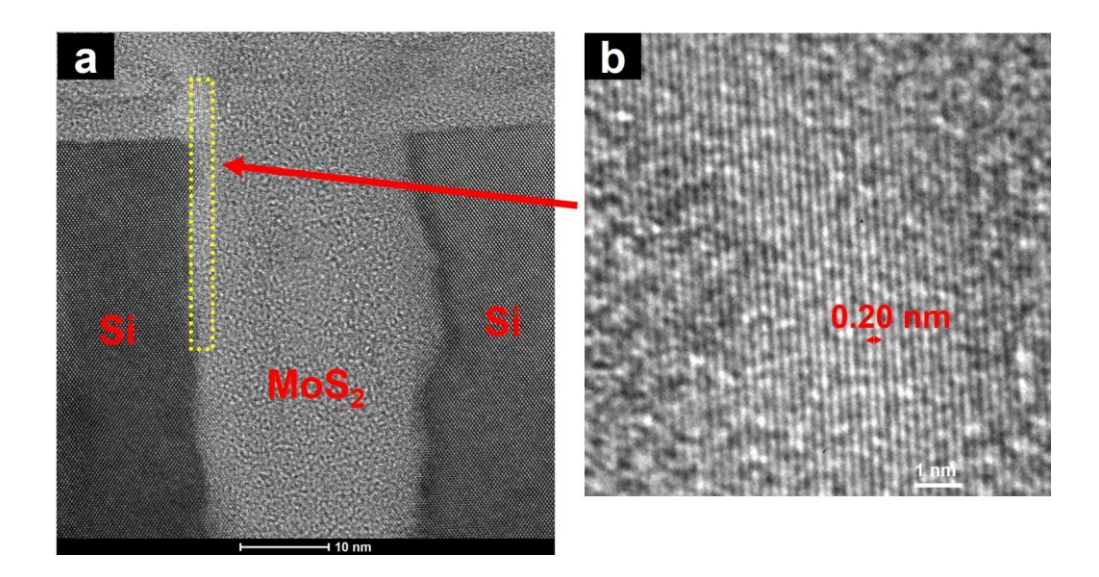


Figure 6. (a) HRTEM micrograph of the MoS_2 film grown in a nanoscale silicon hole after being annealed at 800 °C for 8 min; (b) the enlarged view of the MoS_2 film at the wall interface of hole, showing crystalline structure with a distance of about 0.2 nm between two lines.

Figure 6(a) shows the HRTEM micrograph of the MoS₂ film after being annealed at 800 °C in the environment of argon gas for 8 min, Figure 6(b) is an enlarged view of the MoS₂ film at the wall interface of the hole, showing the crystalline structure with a distance of about 0.2 nm between two lines.

Figure 7(a) shows the cross-sectional HRTEM micrograph of the MoS_2 film after being annealed at 900 °C in the environment of argon for 8 min; Figure 7(b) is an enlarged view of MoS_2 film at the exit of the hole, showing the crystalline structure with a distance of about 0.55 nm between two lines; Figure 7(c) is an enlarged view of MoS_2 film on the substrate surface outside the hole, showing the crystalline structure with a distance of about 0.27 nm between two lines; Figure 7(d) is an enlarged view of MoS_2 film in the hole, showing the crystalline structure with a distance of

about 0.22 nm between two lines; All these local crystalline structures were formatted randomly during the high-temperature annealing

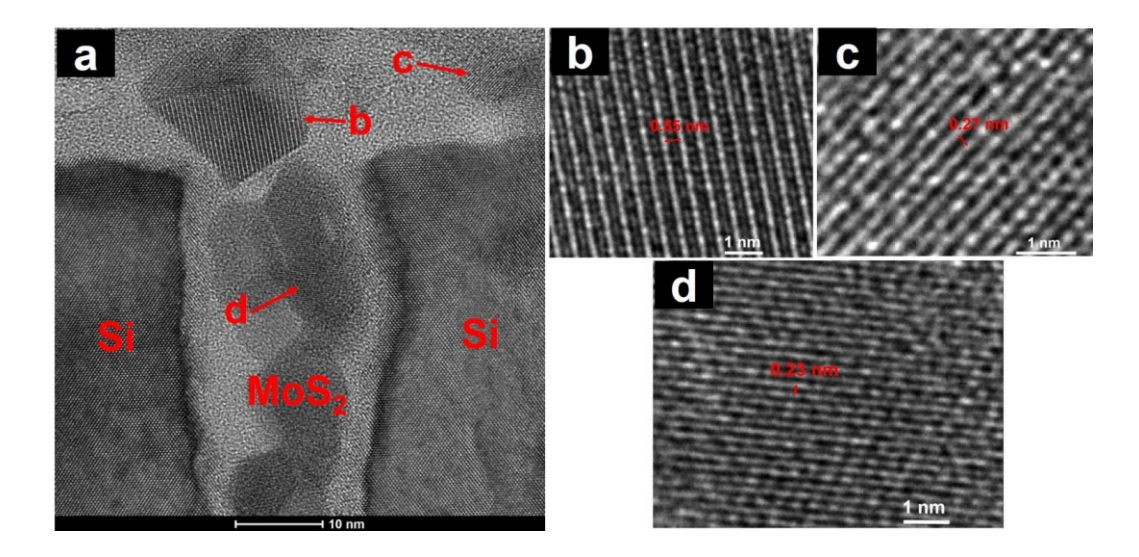


Figure 7. (a) HRTEM micrograph of the MoS₂ film after being annealed at 900 °C for 8 min; (b) the enlarged view of MoS₂ film at the exit of the hole marked by "b" in Figure 7(a), showing the crystalline structure with a distance of about 0.55 nm between two lines; (c) the enlarged view of MoS₂ film on the substrate surface outside the hole marked by "c", showing the crystalline structure with a distance of about 0.27 nm between two lines; (d) the enlarged view of MoS₂ film in the hole marked by "d", showing the crystalline structure with a distance of about 0.23 nm between two lines. process, however, they are compatible with those observed in the MoS₂ film and reported by other researchers [13, 18, 19].

Table I shows that the MoS_2 film has 18% Mo, 36% S, 15% Si, 17% C, and 14% O. The Si and O are from the silicon substrate while the C is from the surface of the film. The XPS analysis indicates that the MoS_2 film has the stoichiometric ratio of 1 (Mo: 18%) to 2 (S: 36%).

Table I. Compositions in the MoS₂ film

Atomic Concentration (%) of MoS ₂ Film				
Mo	S	Si	С	0
18	36	15	17	14

Figure 8 shows the XPS scan of S $2p^{1/2}$ and $2p^{3/2}$ in the MoS₂ film. Figure 9(a) shows the XPS scan of Mo $3p^1$ and $3p^2$ in the MoS₂ film while Figure 9(b) shows the XPS scan of Mo $3d^{3/2}$ and $3d^{5/2}$ in the MoS₂ film. All the peaks in the XPS spectroscopy have the right corresponding binding energy for the Mo and S elements of MoS₂ [20, 21].

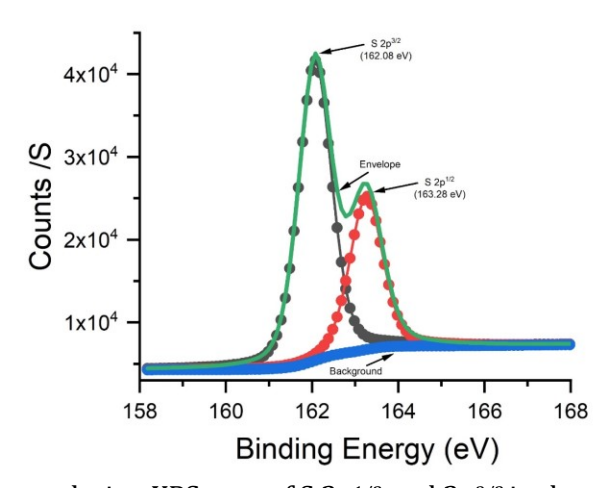


Figure 8. High-resolution XPS scan of S $2p^{1/2}$ and $2p^{3/2}$ in the grown MoS₂ film.

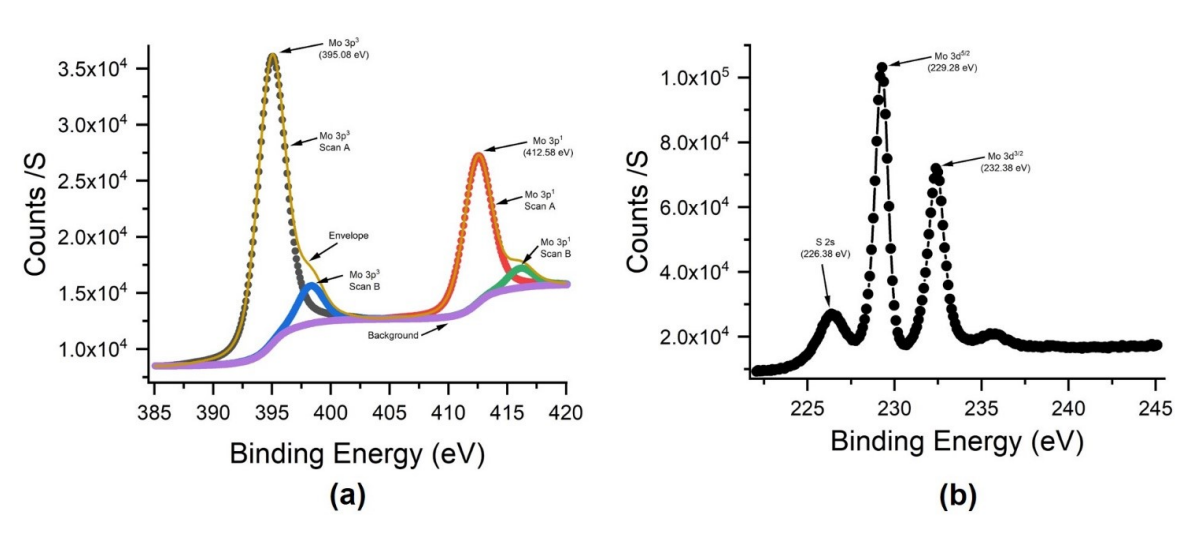


Figure 9. (a) High-resolution XPS scan of Mo $3p^1$ and $3p^2$ in the grown MoS₂ film; (b) High-resolution XPS scan of Mo $3d^{3/2}$ and $3d^{5/2}$ in the grown MoS₂ film.

Figure 10(a) shows the Raman spectrum of the MoS_2 film on the nanoscale hole-patterned silicon substrate and Figure 10(b) is an optical micrograph of the mapping area during the Raman measurement.

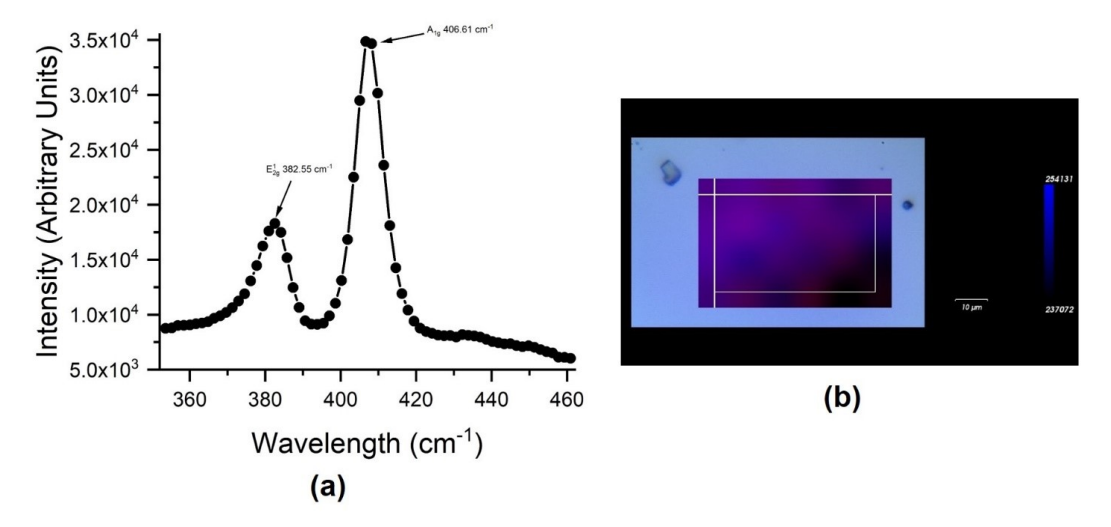


Figure 10. (a) Raman spectrum of the MoS_2 film grown on the nanoscale hole-patterned silicon substrate, showing that the measurement has the E^{1}_{2g} and A_{1g} peaks in the grown MoS_2 film; (b) the optical micrograph of the mapping area.

The Raman spectrum (Figure 10(a)) shows that the measurement has the E^{1}_{2g} and A_{1g} peaks in the grown MoS₂ film, where the separation between the two vibrating modes, $E^{1}_{2\Box}$ and A_{1g} , is 24.06 cm⁻¹. The vibration mode of Mo-S bond ($E^{1}_{2\Box}$) along the base in-plane is observed at 382.55 cm⁻¹ and vibration of sulfur along the out-of-plane (A_{1g}) is observed at 406.61 cm⁻¹. The Raman spectra are compatible to those obtained from the MoS₂ film by other researcher [13, 19, 19].

4. Conclusions

Nanostructured molybdenum disulfide (MoS₂) thin films were grown on a nanoscale holepatterned silicon substrate using the plasma-enhanced atomic layer deposition (ALD). The nanoscale hole fabricated with the self-assembly-based nanofabrication method has a diameter of about 20 nm - 30 nm on the top with an inverted pyramid-like bottom and the depth of the nanoscale holes is about 120 nm - 160 nm. Hydrogen sulfide (H₂S) was used as the S source in the growth of molybdenum disulfide (MoS₂) while molybdenum (V) chloride (MoCl₅) powder was used as the Mo source. The MoS₂ film had the stoichiometric ratio of 1 (Mo) to 2 (S) with the right corresponding binding energy and had the E12g and A1g peaks. It was found that the MoS2 film grown in the nanoscale hole, especially at the wall surface of the nanoscale holes, had more hexagonal-like structures, indicating that the nanoscale holes could enhance the formation of hexagonal-like structures due to the nanoscale space confinement and nanoscale interface. A postgrowth high-temperature annealing of the MoS₂ film produced some local crystalline structures in the film randomly, which are compatible with those reported by other researchers. The growth of MoS₂ film on the nanoscale hole-patterned substrate is interesting, according to the finding in this work that more hexagonal-like structures appeared at the wall of holes, when the nanoscale hole becomes narrower, more hexagonal-like nanostructures could be formed in the hole. The electronic device based on the PE-ALD-grown MoS₂ film such as field-effect transistors (FETs) will be fabricated and the electrical property of the MoS₂ film will then be studied in the following research.

Author Contributions: Z.X. designed the experiments, fabricated the materials, analyzed the data, and wrote the manuscript; G.D. performed the fabrication of the nanoscale hole-patterned silicon wafer, analyzed the nanoscale holes and contributed to analyzing the data and writing the manuscript; K.K. performed the HRTEM experiment and contributed to analyzing the data and writing the manuscript; A.J. performed the growth of the material and contributed to analyzing the

data and writing the manuscript; R.M. performed the Raman and XPS experiments and

contributed to analyzing the data and writing the manuscript.

Supplementary Material: See supplementary material for the HRTEM micrograph of the MoS₂ film

grown in nanoscale silicon holes.

Acknowledgements: Research carried out in part at the Center for Functional Nanomaterials,

Brookhaven National Laboratory, which is supported by the U.S. Department of Energy, Office of

Basic Energy Sciences, under Contract No. DE-SC00112704; the research is supported by National

Science Foundation under Grant No. ECCS-2105388 and Department of Defense under Grant No.

W911NF-18-1-0444 and W911NF-17-1-0474.

Data availability statement: All data that support the findings of this study are included within the

article (and any supplementary files).

Conflicts of Interest: The authors declared no conflicts of interest.

References

1. G. Fiori, F. Bonaccorso, G. Iannaccone, T. Palacios, D. Neumaier, A. Seabaugh, S. K. Banerjee, and

L. Colombo, "Electronics based on two-dimensional materials", Nat. Nanotechnol., Vol. 7, 768–779

(2014).

 $^{\circ}$

- 2. M. Chhowalla, D. Jena, and H. Zhang, "2D semiconductors for transistors", Nat. Rev. Mater., Vol. 1, 16052 (2016).
- 3. Q. Qian, J. Lei, J. Wei, Z. Zhang, G. Tang, K. Zhong, Z. Zheng, and K. Chen, "2D materials as semiconducting gate for field-effect transistors with inherent over-voltage protection and boosted ON-current", NPJ 2D Mater. Appl., Vol. 3, 24 (2019).
- 4. S. Conti, L. Pimpolari, G. Calabrese, R. Worsley, S. Majee, D. Polyushkin, M. Paur, S. Pace, D. Keum, F. Fabbri, G. Iannaccone, M. Macucci, C. Coletti, T. Mueller, C. Casiraghi, and G. Fiori, "Low-voltage 2D materials-based printed field-effect transistors for integrated digital and analog electronics on paper", Nature Commun., Vol. 11, 3566 (2020).
- 5. Y. Liu, U. Halim, M. Ding, Y. Liu, Y. Wang, C. Jia, P. Chen, X. Duan, C. Wang, F. Song, M. Li, C. Wan, Y. Huang, and X, Duan1, "Solution-processable 2D semiconductors for high performance large-area electronics", Nature, Vol. 562, 254-258 (2018).
- 6. C. Liu, H. Chen, S. Wang, Q. Liu, Y. Jiang, D. Zhang, M. Liu, and P. Zhou "Two-dimensional materials for next-generation computing technologies", Nature Nanotechnol. Vol. 15, 545–557 (2020).
- 7. S. Najmaei, Z. Liu, W. Zhou, X. Zou, G. Shi, S. Lei, B. I. Yakobson, J. -C. Idrobo, P. M. Ajayan, and J. Lou, "Vapour phase growth and grain boundary structure of molybdenum disulphide atomic layers", Nat. Mater., Vol. 12, 754—759 (2013).
- 8. A. M. van der Zande, P. Y. Huang, D. A. Chenet, T. C. Berkelbach, Y. You, G. Lee, T. F. Heinz, D. R. Reichman, D. Muller, J. C. Hone, "Grains and grain boundaries in highly crystalline monolayer molybdenum disulphide", Nat. Mater., Vol. 12, 554–561 (2013).

- 9. H. Schmidt, S. Wang, L. Chu, M. Toh, R. Kumar, W. Zhao, A. H. Castro Neto, J. Martin, S. Adam, B. Özyilmaz, et al., "Transport properties of monolayer MoS₂ grown by chemical vapor deposition", Nano Lett., Vol. 14, 1909–1913 (2014).
- 10. Z. Xiao, K. Kisslinger, and R. Monikandan, "Atomic layer deposition of nanolayered carbon films", Carbon, Vol. 7, 67 (2021).
- 11. Z. Xiao, K. Kisslinger, S. Chance, and S. Banks, "Comparison of hafnium dioxide and zirconium dioxide grown by plasma-enhanced atomic layer deposition for the application of electronic materials", Crystals, Vol. 10, 136 (2020).
- 12. A. Valdivia, D. J. Tweet, and J. F. Conley Jr, "Atomic layer deposition of two dimensional MoS₂ on 150 mm substrates", J. Vac. Sci. Technol., Vol. 34, 021515-1-5 (2016).
- 13. Z. Jin, S. Shin, D. Kwon, S. Hana, and Y. Min, "Novel chemical route for atomic layer deposition of MoS2 thin film on SiO₂/Si substrate", Nanoscale, Vol. 6, 14453-14458 (2014).)
- 14. G. S. Doerk and K. G. Yager, "Rapid ordering in "wet brush" block copolymer/homopolymer ternary blends", ACS Nano, Vol. 11, 12326–12336 (2017).
- 15. G. S. Doerk, R. Li, M. Fukuto, A. Rodriguez, and K. G. Yager, "Thickness-dependent ordering kinetics in cylindrical block copolymer/homopolymer ternary blends", Macromolecules, Vol. 51, 10259–10270 (2018).
- 16. K. Toth, S. Bae, C. O. Osuji, K. G. Yager, and G. S. Doerk, "Film thickness and composition effects in symmetric ternary block copolymer/homopolymer blend films: Domain spacing and urientation", Macromolecules, Vol. 54, 7970–7986 (2021).

 \cup

- 17. A. A. Kulkarni and G. S. Doerk, "Hierarchical, self-assembled metasurfaces via exposure-controlled reflow of block copolymer-derived nanopatterns", ACS Appl. Mater. Interfaces, Vol. 14, 27466–27475 (2022).
- 18. L. K. Tan, B. Liu, J. H. Teng, S. Guo, H. Y. Low, and K. P. Loh, "Atomic layer deposition of a MoS2 film", Nanoscale, Vol. 6, 10584 (2014).
- 19. Y. H. Lee, X. Q. Zhang, W. Zhang, M. T. Chang, C. T. Lin, K. D. Chang, Y. C. Yu, J. T. W. Wang, C. S. Chang, L. J. Li, and T. W. Lin, "Synthesis of large-area MoS2 atomic layer with chemical vapor deposition", Adv. Mater., Vol. 24, 2320 (2012).
- 20. N. P. Kondekar, M. G. Boebinger, E. V. Woods, and M. T. McDowell, "In situ XPS investigation of transformations at crystallographically oriented MoS₂ interfaces", ACS Appl. Mater. Interfaces, Vol. 9, 32394–32404 (2017).
- 21. J. Wang, J. Chen, W. Lu, M. Zeng, L. Tan, F. Ren, C. Jiang, and L. Fu, "Direct growth of molybdenum disulfide on arbitrary insulating surfaces by chemical vapor deposition", RSC Adv., Vol. 5, 4364-4367 (2015).